

Spectral Hardness Decay with Respect to Fluence in BATSE Gamma-Ray Bursts

A. Crider and E. P. Liang

Department of Space Physics and Astronomy, 6100 S. Main, Rice University, Houston, TX 77005-1892

R. D. Preece, M. S. Briggs, G. N. Pendleton, and W. S. Paciesas

Department of Physics, University of Alabama in Huntsville, Huntsville, AL 35899

and

D. L. Band and J. L. Matteson

Center for Astrophysics and Space Sciences 0424, University of California at San Diego, La Jolla, CA 92093

ABSTRACT

We have analyzed the evolution of the spectral hardness parameter, E_{pk} (the maximum of the νF_{ν} spectrum) as a function of fluence in gamma-ray bursts. We fit 41 pulses within 26 bursts with the trend reported by Liang & Kargatis (1996) which found that E_{pk} decays exponentially with respect to photon fluence $\Phi(t)$. We also fit these pulses with a slight modification of this trend, where E_{pk} decays linearly with energy fluence. In both cases, we found the set of 41 pulses to be consistent with the trend. For the latter trend, which we believe to be more physical, the distribution of the decay constant Φ_0 is roughly log-normal, where the mean of $\log_{10}\Phi_0$ is 1.75 ± 0.07 and the FWHM of $\log_{10}\Phi_0$ is 1.0 ± 0.1 . Regarding an earlier reported invariance in Φ_0 among different pulses in a single burst, we found probabilities of 0.49 to 0.84 (depending on the test used) that such invariance would occur by coincidence, most likely due to the narrow distribution of Φ_0 values among pulses.

Subject headings: gamma-ray: bursts, observations

1. Introduction

The discovery of a gamma-ray burst optical counterpart with a measurable redshift seems to have shown that the sources are cosmological in origin (Djorgovski et al. 1997, Metzger et al. 1997). The observed fading multi-wavelength afterglows are so far consistent with the simple relativistic blastwave model (Mészáros & Rees 1997) which radiates via a synchrotron shock. However, the emission mechanism resulting in the prompt gamma rays remains a mystery. Studies of gamma-ray burst (GRB) spectral evolution have uncovered many trends which may be used to test possible emission mechanisms. In general, studies of GRB spectral evolution have focused on the “hardness” of bursts, measured either by the ratio between two detector channels or with more physical variables such as the spectral break or peak power energy E_{pk} (Ford et al. 1995) which is the maximum of νF_{ν} , where ν is photon energy and F_{ν} is the specific energy flux. Such hardness parameters were found to either follow a “hard-to-soft” trend (Norris et al. 1986), decreasing monotonically while the flux rises and falls, or to “track” the flux during GRB pulses (Golenetskii et al. 1983, Kargatis et al. 1994).

The discovery that E_{pk} often decays exponentially in bright, long, smooth BATSE GRB pulses *as a function of photon fluence* $\Phi (= \int_{t'=0}^{t'=t} F_N(t') dt')$ (Liang & Kargatis 1996, hereafter

LK96) provided a new constraint for emission models (Liang et al. 1997, Liang 1997, Daigne & Mochkovitch 1998). In their analysis, LK96 fit the function

$$E_{\text{pk}}(t) = E_{\text{pk}(0)} e^{-\Phi(t)/\Phi_0^{\text{LK}}} \quad (1)$$

to 37 GRB pulses in 34 bursts. To interpret this empirical trend, they differentiated Eq. 1 to find

$$-dE_{\text{pk}}/dt = E_{\text{pk}} F_N/\Phi_0^{\text{LK}} \approx F_E/\Phi_0^{\text{LK}} \quad (2)$$

where $F_E = \int_{E \approx 30 \text{ keV}}^{E \approx 2000 \text{ keV}} E N(E) dE$ is the BATSE energy flux (see Eq. 1 of LK96). In this paper, we wished to avoid the assumption that $E_{\text{pk}} F_N \approx F_E$. To do this, we directly tested the trend $-d(E_{\text{pk}})/dt = F_E/\Phi_0$ by integrating it to give us the function

$$E_{\text{pk}}(t) = E_{\text{pk}(0)} - \mathcal{E}(t)/\Phi_0 \quad (3)$$

where $\mathcal{E}(t)$ ($= \int_{t'=0}^{t'=t} F_E(t') dt'$) is the BATSE energy fluence. We emphasize that this is not a fundamentally different trend from the form used in LK96.

The decay constant Φ_0^{LK} appeared to be invariant among pulses during some bursts analyzed in LK96, suggesting that individual pulses in a burst may originate in the same plasma. These discoveries coupled with the observed evolution of the spectral shape (Crider, Liang & Preece 1998a) suggested that saturated inverse Comptonization may be a viable mechanism during the gamma-ray active phase of bursts (Liang et al. 1997), regardless of the distance scale (Liang 1997).

2. Procedures

To determine the evolution of GRB spectral shapes, we examined High Energy Resolution data collected from the BATSE Large-Area Detectors (LADs) and Spectroscopy Detectors (SDs) on board the Compton Gamma-Ray Observatory (Fishman et al. 1989). We began with the 126 bursts which appear in Preece et al. 1998. These bursts were chosen for having a BATSE fluence (28-1800 keV) $> 4 \times 10^{-5} \text{ erg cm}^{-2}$ or a peak flux (50-300 keV on a 256-ms time scale) $> 10 \text{ photon s}^{-1} \text{ cm}^{-2}$. The counts from the detector most nearly normal to the line of sight of each burst (burst angle closest to 0) were background-subtracted and binned into time intervals each with a SNR of ~ 45 within the 28 keV to 1800 keV range. Such a SNR has been found to be necessary in time-resolved spectroscopy of BATSE gamma-ray bursts (Preece et al. 1998).

We deconvolved the gamma-ray spectra of each time interval using the Band et al. (1993) GRB function

$$\begin{aligned} N_E(E) &= A \left(\frac{E}{100 \text{ keV}} \right)^\alpha \exp \left(-\frac{E}{E_0} \right), & (\alpha - \beta)E_0 \geq E, \\ &= A \left[\frac{(\alpha - \beta)E_0}{100 \text{ keV}} \right]^{\alpha - \beta} \exp(\beta - \alpha) \left(\frac{E}{100 \text{ keV}} \right)^\beta, & (\alpha - \beta)E_0 \leq E, \end{aligned} \quad (4)$$

where A is the amplitude (in photon $\text{s}^{-1} \text{ cm}^{-2} \text{ keV}^{-1}$) and $E_0 = E_{\text{pk}}/(2 + \alpha)$. While LK96 assumed that α and β were constant during the course of each burst, this has since been shown to be untrue with a larger data set. (Crider et al. 1997). We thus left α and β as free parameters in our fits.

At this point, we needed to select pulses within our bursts that we could use to test Equations 1 and 3. Ideally, our pulses would not overlap other pulses and our method for choosing the time

bins associated with a pulse would not be biased. Unfortunately, by forcing our time bins to have a $\text{SNR} \sim 45$ so that spectra may be fit to them, much time resolution is lost. Pulses which would be easily separable at a higher time resolution become blurred together. In Figure 1, we show an example of what would likely be identified as two pulses in our coarse ($\text{SNR} \sim 45$) data. Below it, 64-ms count rate data for this same burst, obtained from the Compton Observatory Science Support Center (COSSC), is plotted. With higher time resolution, we see this bursts is composed of at least 4 distinct pulses.

To avoid contaminating our sample with overlapping pulses (and to avoid biases introduced by a human in pulse selection), we used the COSSC 64-ms count rates and background fits to determine where each of our pulses began and ended. To do this, we developed an interactive IDL routine to fit the Norris et al. (1996) pulse profile to the individual pulses within these bursts. The pulse profile function for the count rate $C(t)$ can be written

$$C(t) = A \exp \left(-\left| \frac{t - t_{\max}}{\sigma_{r,f}} \right|^\nu \right) \quad (5)$$

where t_{\max} is the time of maximum count rate, σ_r and σ_d are the count rate rise and decay time constants, and ν is the pulse “peakedness”. For an exponential rise and decay, $\nu = 1$. When $\nu = 2$ and $\sigma_r = \sigma_d$ this shape describes a Gaussian.

With 64-ms resolution, we found that in many bursts pulses overlapped in a fashion making them too complex for us to fit individual pulses. Other bursts contained pulses which could be resolved, but none of their pulses lasted long enough to span at least 4 time bins with $\text{SNR} \sim 45$. For 13 of the bursts, no processed 64-ms data was available. We discarded bursts which fell into any of these three categories. This left us with 26 bursts. This is comparable to the 34 multi-pulse bursts used in LK96, which included several pulses which appear to be overlapping when confronted with the 64-ms data. To avoid overlap in our own analysis, we used only bins which were dominated by a single pulse (at least 70% of the counts from one pulse). Within our 26 bursts, we identified 41 regions composed of at least 4 time bins dominated by a single pulse. The time bins selected for each pulse were consecutive in all but two cases (BATSE triggers 451 and 3290). The 64-ms data for each of these two bursts suggests that a short pulse occurred near the middle of a longer pulse, which forced us to fit two separate regions with a single decay law.

Our next step was to test the E_{pk} -fluence relations (Equations 1 and 3) with each of the selected pulses. Our motivation for emphasizing the E_{pk} -energy fluence relation (Eq. 3) as opposed the E_{pk} -photon fluence relation (Eq. 1) is that we believe that the former represents a more physical quantity. It is possible (perhaps even likely) that the observed BATSE photon fluence is a poor representation of the bolometric photon fluence. The BATSE LAD energy window was designed to contain the peak of GRB energy spectra, *not* the peak of the photon spectra. By using energy fluence in place of photon fluence, we can avoid the shakier assumption that the BATSE LAD photon flux is proportional to the bolometric photon flux. LK96 had attempted this but found that statistical errors in \mathcal{E} were too large to be useful. This was a result of their fixing α and β in the spectral fitting. When we fit the time-resolved spectra with variable α and β , we obtained much smaller errors for \mathcal{E} , which made testing the $E_{\text{pk}} - \mathcal{E}$ relation possible. Nevertheless, we also fit Eq. 1 to our pulses in this paper both for historical reasons and as a test of our interpretation.

3. Results

We fit both the $E_{\text{pk}} - \Phi$ and the $E_{\text{pk}} - \mathcal{E}$ relations to our 41 clean pulses using FITEXY (Press *et al.* 1992). Table 1 summarizes the results for each of the pulses in our sample. The first column is the BATSE trigger number. The second column is the burst name, which is also the date the burst triggered in the format YYMMDD. The third column is the number of the LAD which was used for processing. The fourth column lists the t_{max} from the Norris function fit to the pulse. The fifth column is the energy fluence within the bins selected for fitting in units MeV cm^{-2} . The sixth column gives the number of bins selected for fitting. The seventh column is the fitted value Φ_0^{LK} for each pulse defined in Eq. 1. The eighth and ninth columns are the fitted values of Φ_0 and $E_{\text{pk}(0)}$ for each pulse as defined in Eq. 3. Of course, Φ_0 will only equal Φ_0^{LK} if $E_{\text{pk}}F_N = F_E$. Since the latter is not strictly true, we find that $\Phi_0 \approx \Phi_0^{\text{LK}}$. For completeness, we also show the plots of E_{pk} versus \mathcal{E} and their fits in Figure 2.

From the χ^2 and the number of fluence bins for each decay fit, we calculated the probability Q of randomly getting a higher χ^2 by chance. Thus, $Q \geq \sim 0.5$ represents very good fits, while $Q \sim 0$ represents poor fits. The Q values from fits of Eq. 3 to our pulses appear in the tenth column of Table 1. If E_{pk} does indeed cool linearly with \mathcal{E} in all pulses selected for fitting, then when plotting the cumulative distribution of Q values, we would expect 10% of the pulses to have a Q less than 0.1, 20% of the pulses to have a Q less than 0.2, and so on. Figure 3 shows the cumulative distribution of Q values for our pulses with acceptable fits. An excess of pulses with very high Q values would suggest a biased pulse selection process. A Kolmogorov-Smirnov test ($P = 0.18$) applied to our distribution of Q values suggests that the set of 41 pulses is not too biased and roughly follows the distribution we would expect if all of them are consistent with a linear decay of E_{pk} with respect to energy fluence.

By fitting the E_{pk} – fluence law to the full observable duration of each pulse and not just the flux decay phase, we could characterize our pulses as “hard-to-soft”. None of our pulses required a “tracking” classification, though many of the ambiguous pulses excluded from this study could be “hard-to-soft” or “tracking”. Three of the pulses in our sample (BATSE triggers 2316, 3491, and 3870) contain pulses with negative values of Φ_0 . However, all three of these pulses are still consistent with a positive value of Φ_0 . We remind the reader here that large absolute values of Φ_0 (like those in these three pulses) correspond to pulses with very little change in E_{pk} , where $\frac{1}{\Phi_0} \equiv \frac{dE_{\text{pk}}}{d\mathcal{E}} \approx 0$. In such cases, small statistical errors in $\frac{dE_{\text{pk}}}{d\mathcal{E}}$ translate to very large statistical errors in Φ_0 . Even if all pulses decay monotonically from hard-to-soft, we should expect to see a few pulses to have negative values of Φ_0 . Since all of our pulses are consistent with a monotonic decay in E_{pk} , we adopt the hypothesis that all pulses behave this way for the remainder of this paper and drop these three pulses from our sample to simplify our calculations.

3.1. Distribution of Φ_0

The distribution of fitted Φ_0 values appears in Figure 4. It is roughly log-normal where the mean of $\log_{10}\Phi_0$ is 1.75 ± 0.07 and the FWHM of $\log_{10}\Phi$ is 1.0 ± 0.1 . This distribution likely suffers some selection effects. This becomes obvious when one realizes that $\Phi_0 \approx -\frac{\Delta\mathcal{E}}{\Delta E_{\text{pk}}}$. We see that the smallest absolute value of Φ_0 is limited by the minimum energy fluence which allows one to fit spectra (about 1 MeV cm^{-2} from Table 1) and the energy window of BATSE (max $\Delta E_{\text{pk}} \approx 1870 \text{ keV}$). There are no such limitations on the high side of this distribution, since $|\Delta E_{\text{pk}}|$ can be arbitrarily small and $\Delta\mathcal{E}$ is only limited by nature.

3.2. Testing the Invariance of Φ_0 Among Pulses within Bursts

LK96 reported that the decay constant Φ_0^{LK} sometimes remains fixed from pulse to pulse within some bursts. Such behavior would hint at a regenerative source rather than a single catastrophic event (such as Mészáros & Rees 1993). However, the intrinsically narrow distribution of decay constants mentioned above and the relatively large confidence regions for each pulse's value of Φ_0 suggest that many bursts would appear to have an invariant decay constant merely by chance.

As done earlier with a larger, but less reliable, set of pulses (Crider, Liang & Preece 1998b), we calculated three statistics for each multi-pulse burst to test the invariance of the E_{pk} – fluence decay constant. We compared two of each bursts' M pulses at a time using the statistic

$$X_{ij}^2 = \frac{[\Phi_0(i) - \Phi_0(j)]^2}{\sigma_{\Phi_0(i)}^2 + \sigma_{\Phi_0(j)}^2} \quad (6)$$

and then distilled the comparisons within each burst into a single statistic to represent that burst. These statistics are defined in Table 2. Each is tailored for different null hypotheses. The statistic G_1 tests if *at least* two pulses in a burst are similar (and thus “invariant”), while G_2 tests if *all* the pulses have a similar decay constant. G_3 tests for either a single good pairing or several moderately close pairings. We believe that this last statistic is the most reasonable for testing our results since it does not require that *all* pulses decay at the same rate (as G_2 does) but also does not discard information about multiple pulses repeating (as G_1 does). Finally, we calculated a table of probabilities $P(G, M)$ for our goodness-of-fit statistics G based on a simple Monte Carlo simulation. We created synthetic bursts with pulse decay parameters randomly sampled from the observed distributions of Φ_0 and σ_{Φ_0}/Φ_0 . To avoid any bias that intrinsic invariances would have on these distributions, we created them using only one pulse from each burst. The sample of bursts in this study has fewer bursts than previous works, and hence has fewer bursts with more than one pulse. The three versions of the G statistic defined above are equivalent when only two pulses appear in a burst. Thus for this sample, with only 3 of the 9 multipulse bursts having more than 2 pulses, these statistics are nearly equivalent. The high probability that the observed repetitions occurred by coincidence leads us to conclude that pulse decays are not invariant from pulse to pulse within bursts. Instead, we suggest that the distribution of Φ_0 values seen in all bursts is narrow enough that an apparent invariance of Φ_0 is inevitable in some burst. We came to the same conclusion when examining Φ_0^{LK} (Crider, Liang & Preece 1998b).

4. Discussion

Out of the 26 bursts to which we could fit a time-evolving Band GRB function, all contain at least one pulse consistent with a linear decay of E_{pk} with respect to energy fluence. Of the 41 pulses in these bursts, all are consistent ($Q > 0.001$; Press *et al.* 1992) with this decay pattern. This is also true when we fit the LK96 exponential decay of E_{pk} with respect to photon fluence. Besides LK96, other quantitative spectral evolution trends have been reported for GRBs. The averaged temporal and spectral evolution for 32 bright GRBs has been calculated in Fenimore 1998. The averaged photon flux evolution can be described as both rising and decaying linearly with time. The hardness, as measured by E_{pk} with α and β held fixed, also appears to decay linearly with time during the averaged burst ($E_{\text{pk}} = E_{\text{pk}(0)}(1 - t/t_0)$). This is clearly not representative of all bursts since the evolution in bursts of E_{pk} is often complex (Ford *et al.* 1995, Liang & Kargatis 1996). These trends possibly reflect the physics dictating the envelope

of emission. The fact that LK96 found the E_{pk} -fluence trend in many mingled pulses may result from the fact that the burst envelope also evolves in this manner.

Since the hardness of this envelope appears to decay more slowly than the hardness during the pulses we observe, we might not expect to see this trend in our pulses. However, the degree of confidence of E_{pk} in our fits, coupled with the fact that energy fluence is often linear in time, makes the observations of many bursts possibly consistent ($Q > 0.001$) with this decay law. Testing the distribution of Q values as we did in Fig 3, we find a probability $P=0.001$ that the pulses are realizations of linear E_{pk} -time trend, compared to $P=0.18$ for the linear E_{pk} -energy fluence trend. While the linear E_{pk} -time relation does not seem to describe individual pulses as well as the E_{pk} -fluence relation, the results are not conclusive.

More pulses are clearly needed if one is to discriminate between any two time-dependent spectral functions. One could simply wait for bursts to occur or for a more sensitive instrument to be built. However, it may be possible to increase the number of fittable pulses using the existing BATSE database. Fitting a time-dependent spectral function directly to higher time resolution data (or time-tagged event data) greatly reduces the number of required fit parameters. Another approach may be to analytically integrate the time-dependent spectral function and fit that to integrated spectra, as has been done by Ryde & Svensson (1998). By increasing the number of pulses, it will become possible to make more definitive statements about the evolution of prompt GRB emission and how it relates to the GRB afterglow.

AC thanks NASA-MSFC for the Graduate Student Research Program fellowship. It is also a pleasure to mention very useful discussions with Ed Fenimore, Charles Dermer, Markus Böttcher, and Rodney Hurley. This work is supported by NASA grant NAG5-3824.

REFERENCES

Band, D., *et al.* 1993, ApJ, 413, 281
Crider, A., Liang, E.P., & Preece, R.D. 1998b, AIP 428, 359
Crider, A., Liang, E.P., & Preece, R.D. 1998a, AIP 428, 63
Crider, A., *et al.* 1997, ApJ, 479, L39
Daigne, F. & Mochkovitch, R. 1998, *astro-ph/9801245*
Djorgovski, S. G., *et al.* 1997, Nature, 387, 876
Fenimore, E.E. 1998, ApJ, submitted, *astro-ph/9712331*
Fishman, G.J., *et al.* 1989, Proc. of the GRO Science Workshop, 2-39
Ford, L.A., *et al.* 1995, ApJ, 439, 307
Golenetskii, S.V., Mazets, E.P., Aptekar, R.L., & Ilyinskii, V.N. 1983, Nature, 306, 451
Kargatis V.E. *et al.* 1994, ApJ, 422, 260
Liang, E.P. & Kargatis V.E. 1996, Nature, 381, 49
Liang, E.P., Smith, I.A., Kusunose, M., & Crider, A. 1997, ApJ, 479, L35
Liang, E.P. 1997, ApJ, 491, L15
Mészáros, P. & Rees M.J. 1997, ApJ, 476, 232
Mészáros, P. & Rees M.J. 1993, ApJ, 405, 278

Metzger, M.R. et al. 1997, *Nature*, 387, 879
Norris, J.P., et al. 1996, *ApJ*, 459, 393
Norris, J.P., et al. 1986, *ApJ*, 301, 213
Preece, R. D. et al., 1998, *ApJ*, 496, 849
Press, W.H., Teukolsky, S.A., Vetterling, W.T., & Flannery B.P., *Numerical Recipes in C*, 2nd Edition, 1992, (Cambridge:Cambridge University)
Ryde, F. & Svensson R. 1998, *ApJ*, (in press)

Fig. 1.— The time history of BATSE trigger 543 seen both in (a) the lower time resolution which allowed us to fit a spectrum to each bin and (b) 64-ms resolution. Count rate is marked in each plot as a histogram and E_{pk} , as determined from the data in the upper plot, is marked on both plots for convenience. While it is clear in the lower plot that there are at least 4 pulses within this burst, only two peaks in flux are evident in the upper plot. The fits of the Norris function (Eq. 5) to these pulses are plotted here as dotted lines.

Fig. 2.— The E_{pk} (crosses) and photon flux (histogram) evolution of 26 gamma-ray bursts with respect to energy fluence. Bins used to calculate the decay rate are marked with solid circles. The best fit decay law also appears. One sigma confidence bars for E_{pk} and energy fluence are shown for each bin.

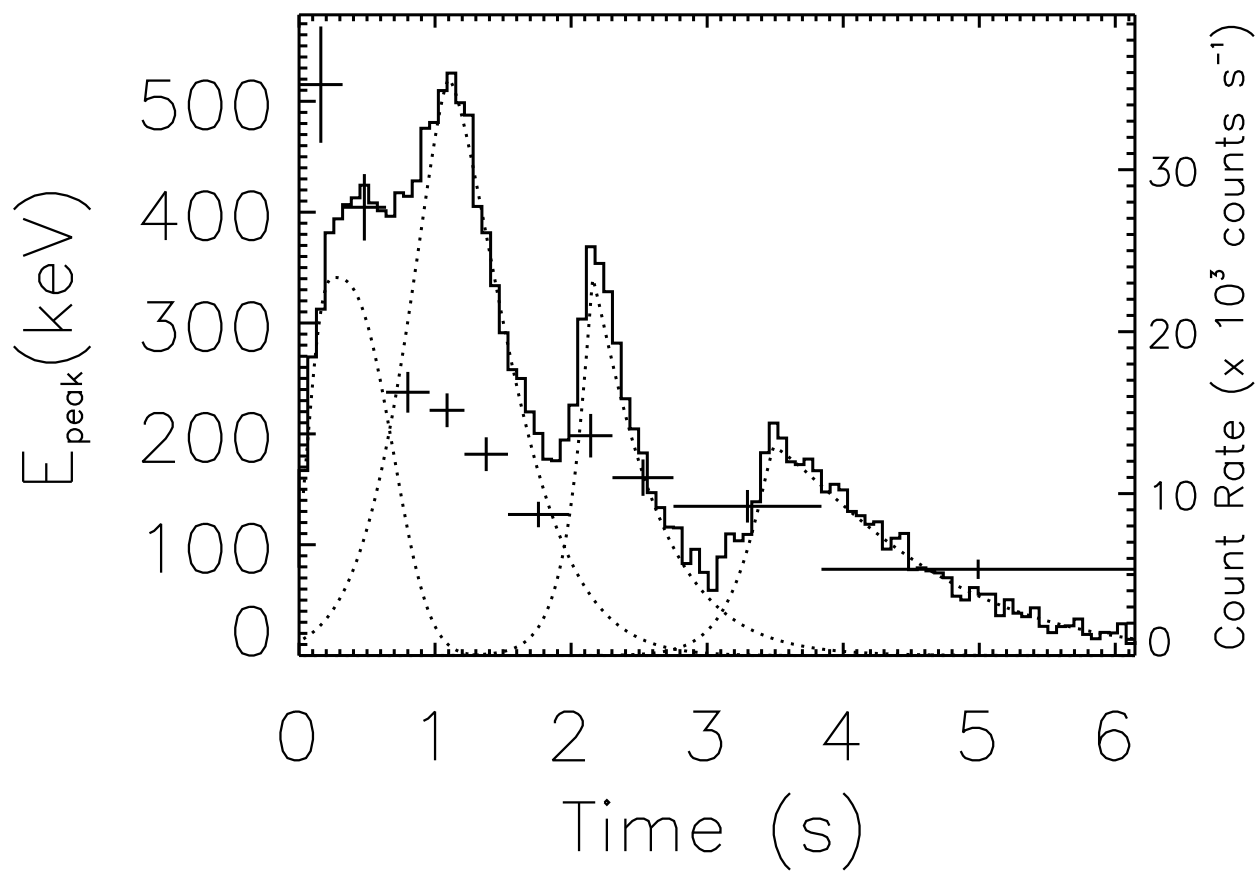
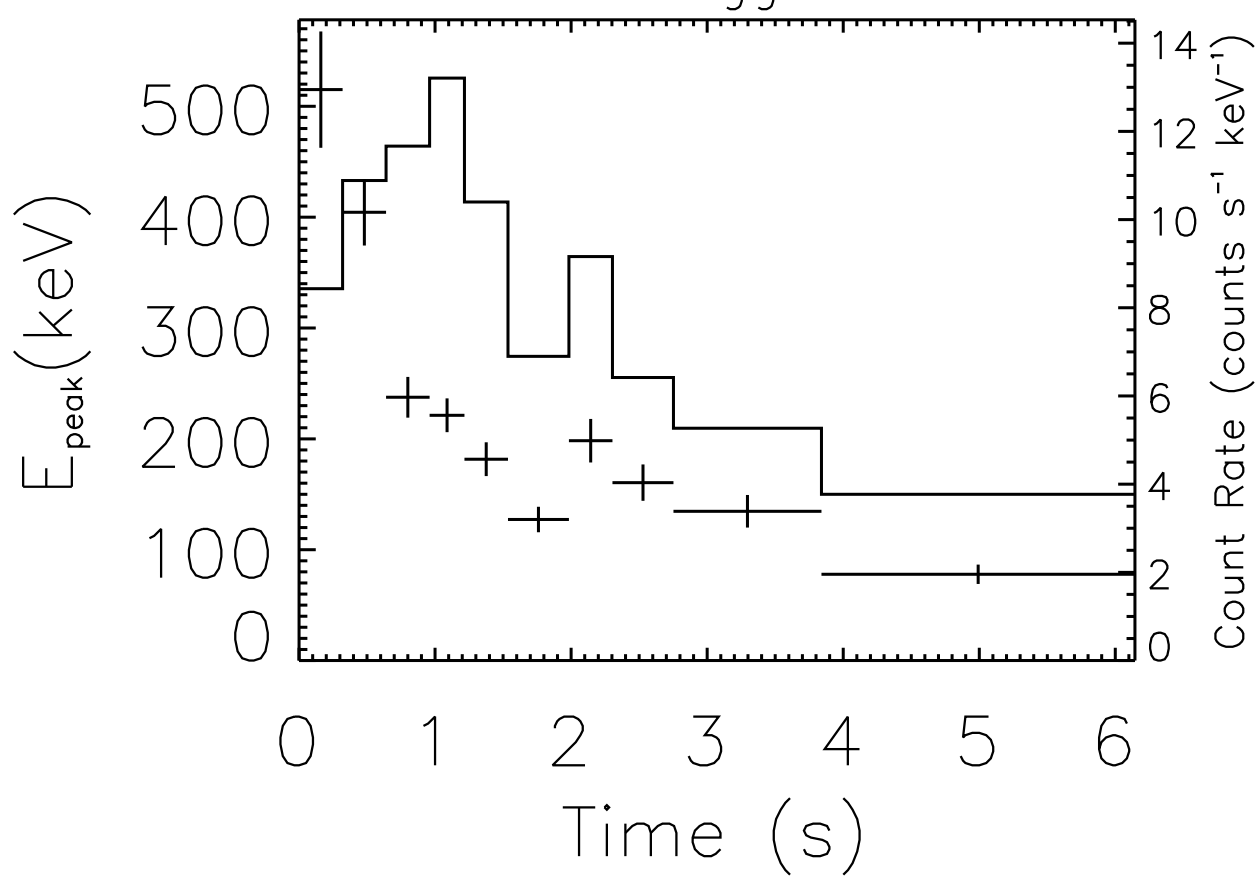
Fig. 3.— Cumulative distribution of Q values for 41 pulses. In this plot, N is the fraction of pulses that have a Q value less than that of a certain pulse. If all of these GRB pulses cooled linearly as a function of energy fluence, one would expect the cumulative Q distribution to match the unit distribution ($N=Q$). The Kolmogorov-Smirnov test gives a probability $P = 0.18$ that this distribution is drawn from the unit distribution. From this, we conclude that our $E_{\text{pk}} - \mathcal{E}$ function (Eq. 3) adequately describes the pulses in this subset.

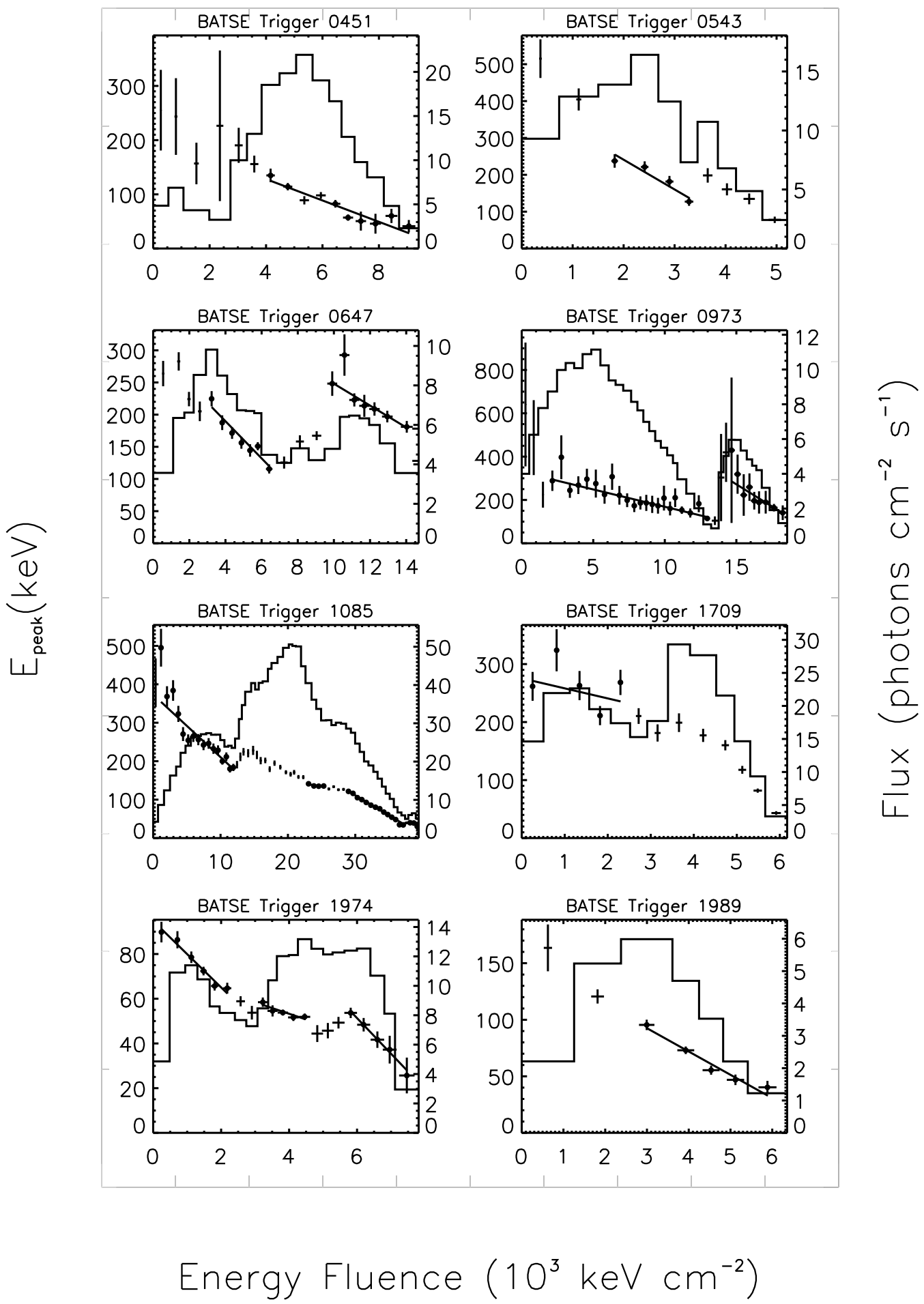
Fig. 4.— This is the distribution of Φ_0 values based on 41 pulses selected from 26 bursts. In this plot, we show both a histogram of values and the best-fit Gaussian distribution. The distribution of Φ_0 values is roughly log-normal where the mean of $\log_{10}\Phi$ is 1.75 ± 0.07 and the FWHM of $\log_{10}\Phi$ is 1.0 ± 0.1 .

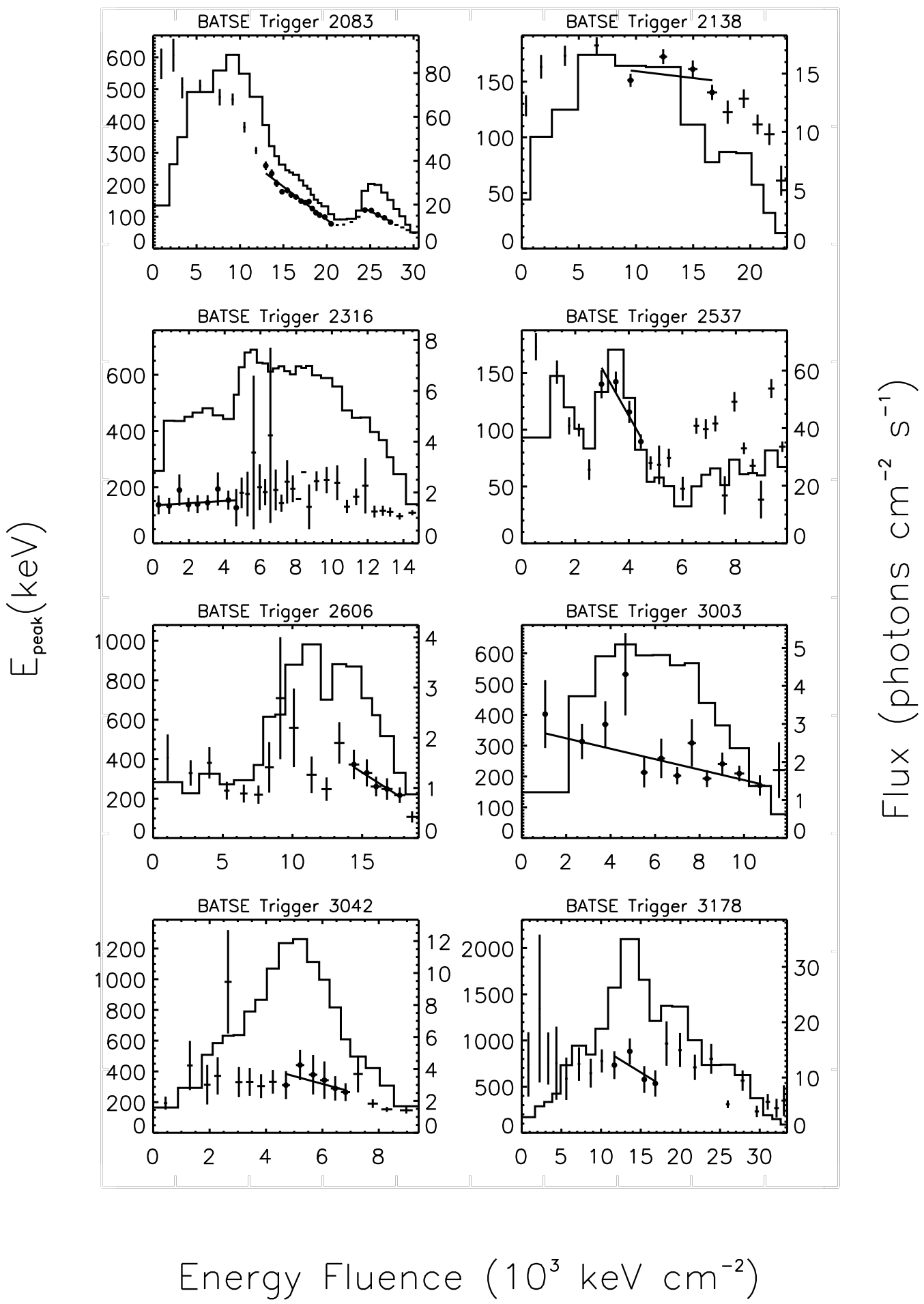
Table 2: The probabilities of getting such good values for each of our three goodness-of-fit statistics G . These probabilities are high enough to suggest that any invariance seen in the data is purely coincidental.

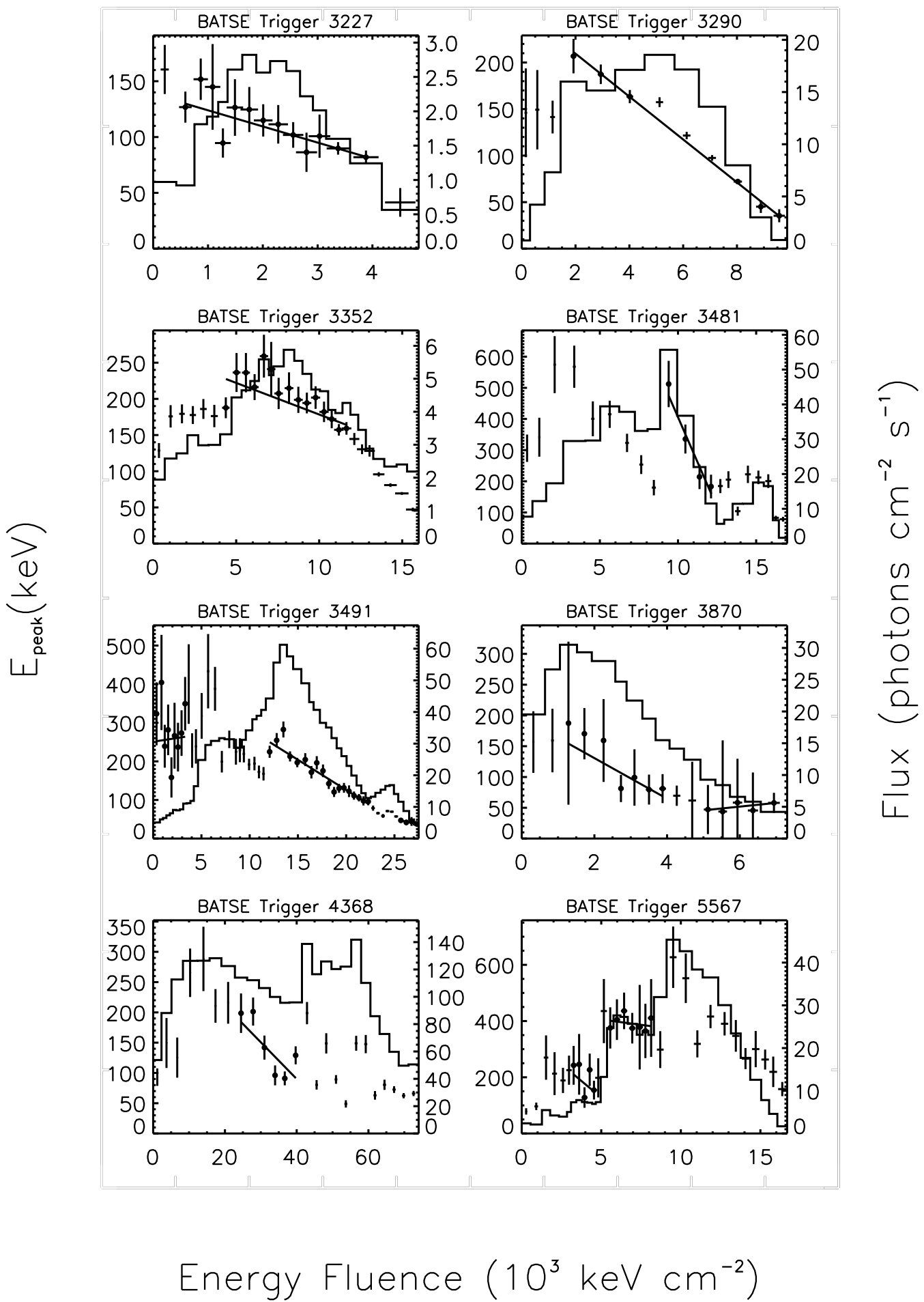
Definition of G_α	$P(G_{\alpha(\text{random})} < G_{\alpha(\text{observed})})$
$G_1 \equiv \min X_{ij}^2$	0.84
$G_2 \equiv \sum_{i=1}^{M-1} \sum_{j=i+1}^M X_{ij}^2$	0.49
$G_3 \equiv \prod_{i=1}^{M-1} \prod_{j=i+1}^M X_{ij}^2$	0.90

BATSE Trigger 543

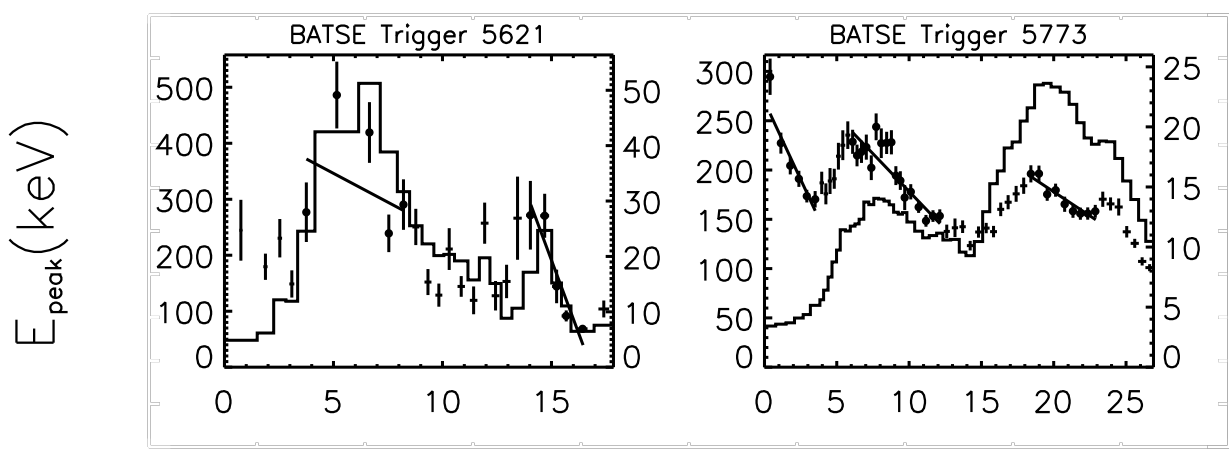




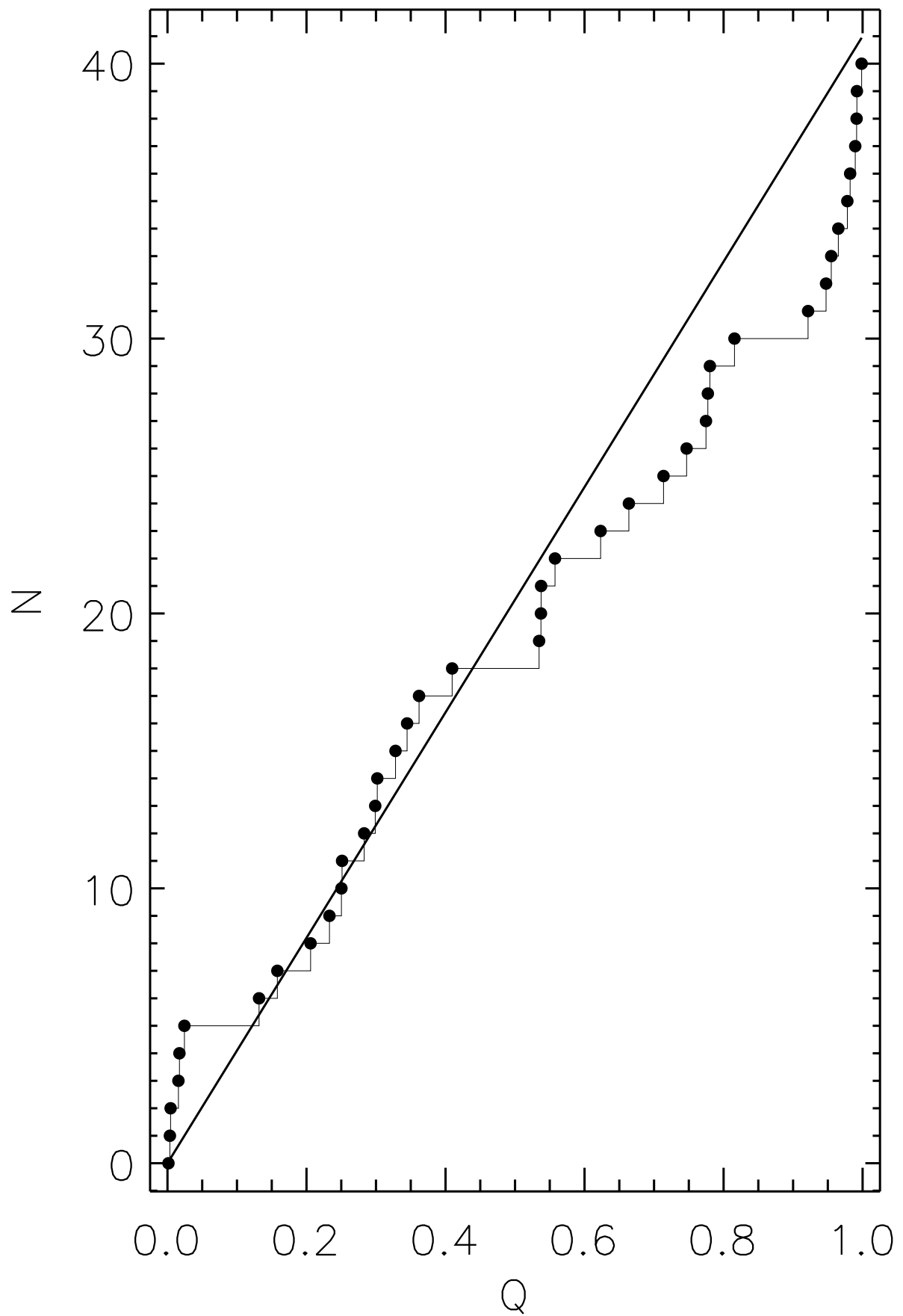




Flux (photons $\text{cm}^{-2} \text{s}^{-1}$)



Energy Fluence (10^3 keV cm^{-2})



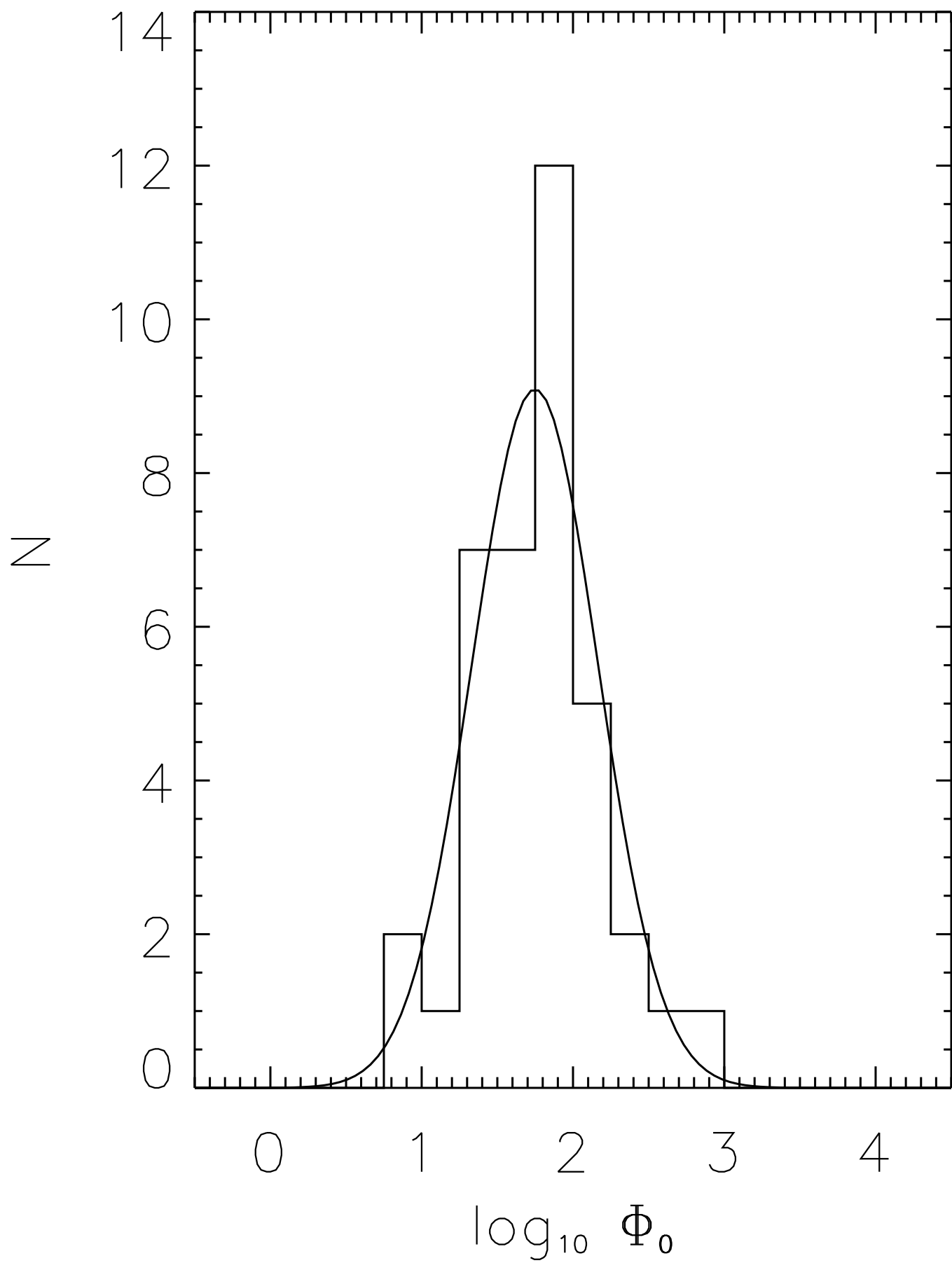


TABLE 1
DECAY PARAMETERS FOR 41 GAMMA-RAY BURST PULSES

BATSE Trigger	Burst Name	LAD	t_{\max} (sec)	$\Delta\mathcal{E}$ (MeV cm $^{-2}$)	Bins	Φ_0^{LK} (cm $^{-2}$)	Φ_0 (cm $^{-2}$)	$E_{\text{pk}(0)}$ (keV)	Q
451	910627	4	5.0	4.9	10	37±5	51±6	125±7	0.206
543	910717	4	1.1	1.5	4	17±3	12±2	255±14	0.251
647	910807	0	14.0	4.1	7	79±17	59±15	249±11	0.664
647	910807	0	3.5	3.2	7	42±5	35±5	212±8	0.299
973	911031	3	2.5	10.8	22	70±9	62±8	295±18	0.965
973	911031	3	23.7	3.6	9	29±10	24±11	285±49	0.991
1085	911118	4	2.5	10.8	16	75±5	61±5	354±10	0.016
1085	911118	4	6.3	2.3	4	564±569	446±462	139±3	0.714
1085	911118	4	9.0	8.1	14	96±3	96±4	121±2	0.992
1085	911118	4	20.2	1.1	3	87±144	140±241	41±9	0.537
1709	920718	7	0.7	2.0	5	130±118	58±49	271±21	0.024
1974	921003	2	1.2	1.9	6	42±6	67±10	91±3	0.775
1974	921003	2	4.6	1.2	5	116±43	196±83	57±2	0.747
1974	921003	2	6.6	1.7	5	26±7	63±19	54±3	0.989
1989	921015	4	117.7	2.9	5	37±4	49±7	93±5	0.535
2083	921207	0	8.5	3.0	5	86±9	74±10	125±4	0.538
2083	921207	0	1.4	7.5	15	61±2	48±2	236±5	0.302
2138	930120	0	78.3	7.1	4	1388±1647	812±805	160±5	0.003
2316	930425	1	4.2	4.4	9	-270±568	-250±566	136±20	0.978
2537	930922	1	1.1	1.5	4	31±6	24±5	155±9	0.233
2606	931026	7	69.8	3.3	5	46±21	22±12	358±54	0.955
3003	940529	0	8.8	9.7	12	70±17	59±19	340±41	0.362
3042	940623	1	7.8	2.1	6	32±25	20±18	383±66	0.816
3178	940921	2	8.0	5.2	4	53±42	19±14	829±111	0.410
3227	941008	5	8.9	3.3	13	42±8	69±16	130±8	0.777
3290	941121	4	38.3	7.7	9	49±2	43±3	211±7	0.947
3352	950111	2	18.1	7.3	15	141±26	114±22	227±9	0.158
3481	950325	2	39.7	2.7	4	13±3	9±2	473±56	0.557
3491	950403	3	7.7	10.2	18	87±6	64±4	250±7	0.283
3491	950403	3	13.2	1.6	4	84±48	191±112	47±3	0.922
3491	950403	3	4.7	3.0	9	-1685±41445	-259±1760	252±48	0.345
3870	951016	5	0.5	2.6	7	20±8	30±17	154±35	0.780
3870	951016	5	2.0	1.8	5	-66±257	-166±612	47±36	0.999
4368	960114	0	18.7	15.2	6	294±69	165±46	184±19	0.004
5567	960807	0	8.7	1.3	5	24±23	21±27	210±60	0.328
5567	960807	0	10.7	2.6	7	322±1680	133±706	401±48	0.982
5621	961001	2	3.9	4.5	5	49±24	48±32	372±43	0.001
5621	961001	2	7.1	2.4	5	11±1	10±2	290±45	0.250
5773	970111	0	8.2	6.0	17	89±7	65±5	238±5	0.017
5773	970111	0	17.2	4.5	9	149±25	103±19	193±5	0.623
5773	970111	0	3.9	3.1	6	34±4	32±5	257±10	0.132